Malaysian Journal of Analytical Sciences (MJAS) Published by Malaysian Analytical Sciences Society



MODELING THE TIME RESPONSE OF CURRENT USING INTERDIGITATED ARRAYS IN A SHALLOW ELECTROCHEMICAL CELL

(Pemodelan Respons Arus Mengunakan Susunan Interdigital dalam Sel Elektrokimia Cetek)

Cristian F. Guajardo Yévenes^{1,2,*} and Werasak Surareungchai^{3,4}

¹Biological Engineering Program, Faculty of Engineering, ²Pilot Plant Development and Training Institute, ³Nanoscience and Nanotechnology Graduate Program, ⁴School of Bioresources and Technology. King Mongkut's University of Technology Thonburi, 49 Soi Thian Thale 25, Thanon Bang Khun Thian Chai Thale Bangkok 10150, Thailand

*Corresponding author: cristian.gua@kmutt.ac.th

Received: 9 February 2022; Accepted: 25 July 2022; Published: 27 December 2022

Abstract

The interdigitated array of electrodes (IDAE) is a common choice for integration in small electrochemical sensors due to the amplified currents and fast response times. The design and assessment of IDAE performance in microfluidic cells require the use of mathematical models, in which the diffusion equation is widely applied. Analytical solutions for this equation are available for IDAEs in tall cells; however, they are not currently available for shallow cells, as is the case with microfluidic devices. The issue of whether it is possible to model the time response of IDAEs in shallow cells using simple exponential functions is addressed in this work. This is achieved by numerically solving the diffusion equation to obtain the time response of the current and later by applying non-linear regression to obtain exponential models. The current response is generally complex due to the many Fourier harmonics involved. However, the findings reveal that when the elapsed time is greater than some characteristic time, the current response can be approximated by an exponential curve. Furthermore, higher currents can be obtained at the expense of longer response times when the cell is tall, while shorter response times can be obtained at the expense of lower currents when the cell is shallow.

Keywords: Shallow electrochemical cell, Interdigitated arrays, Numerical simulation, Current response.

Abstrak

Elektrod susunan interdigital (IDEA) adalah pilihan biasa bagi intergrasi dalam sensor elektrokimia kecil berdasarkan arus teramplikasi dan respons masa yang pantas. Rekabentuk dan penilaian bagi prestasi IDEA di dalam sel mikrobendalir memerlukan pemodelan matematik, di mana persamaan resapan digunakan secara meluas. Penyelesaian analitikal bagi persamaan ini sesuai

Guajardo Yévenes et al.: MODELING THE TIME RESPONSE OF CURRENT USING INTERDIGITATED ARRAYS IN A SHALLOW ELECTROCHEMICAL CELL

bagi IDEA dalam sel tinggi; namun belum ada bagi sel cetek, khusus bagi kes bersama mikrobendalir. Isu terhadap kebarangkalian ia berhasil terhadap model respons masa di dalam sel cetek menggunakan fungsi eksponen mudah telah dikaji. Ia dicapai melalui penyelesaian berangka persamaan resapan untuk mendapatkan respons masa bagi arus dan kemudian digunakan bagi regresi tak linear untuk mendapatkan model eksponen. Respons arus secara umum adalah kompleks disebabkan oleh penglibatan harmonik Fourier. Namun, hasil kajian mendapati apabila masa berlalu lebih kuat berbanding masa pencirian, responsa arus boleh dianggar oleh lengkung eksponen. Selanjutnya, arus yang tinggi boleh diperolehi pada masa respons yang lebih lama apabila susunan sel adalah tinggi, sebaliknya masa respons yang lebih pendek diperolehi pada arus yang rendah di mana kedudukan sel adalah cetek.

Kata kunci: sel elektrokimia cetek, susunan interdigital, simulasi berangka, respons arus

Introduction

Microelectrodes are of interest in electrochemical detection due to their fast response, high current density, and reduced sample volumes [1]. Among these, the interdigitated array of electrodes (IDAE) is a common choice for integration in microfluidic electrochemical sensors due to the amplified currents obtained by redox cycling at multiple electrode bands and the fact that microfluidic devices and microelectrodes share similar fabrication techniques [2, 3].

Obtaining good designs or assessing the performance of IDAE in microfluidic electrochemical cells requires the use of mathematical models. In particular, the diffusion equation is a commonly used model and valid when the effects of convection and migration in the cell are negligible. An analytical solution of the diffusion equation is possible for IDAEs in very tall cells [4]; however, this is not currently available for shallow cells, as in the case of many microfluidic cells. For this reason, numerical simulations of the diffusion equation are commonly performed to obtain the concentration profile and subsequently the current through the cell for the device in question [5, 6].

The issue of whether it is possible to model the time response of the current using simple exponential functions is addressed in this research. This is achieved by numerically solving the diffusion equation for electrochemical cells of different heights containing an IDAE with bands and gaps of equal width. Once this has been done, non-linear regressions are performed on the simulated currents to obtain their fitting parameters, which correspond to the magnitude in steady state and

the time constant (reciprocal of the exponential decay constant). The obtained exponential approximations are valid when the elapsed time is greater than some characteristic times. This model for the current shows that there is a trade-off between faster time responses and higher detection currents, depending on the dimensions of the electrochemical cell and IDAE.

Materials and Methods

Model of the IDAE

Consider an IDAE located at the bottom of an electrochemical cell of height H (Figure 1a). The IDAE consists of two band arrays, A (black) and B (gray), where consecutive bands are separated by the distance W between their centers, have widths of w_A and w_B , and share a common length L which is in contact with the electrochemical solution in the channel. The electrochemical cell may also include a counter electrode, external to the IDAE, when each array is potentiostated independently with a bipotentiostat.

The solution comprises a mixture of oxidized (O) and reduced (R) species, in uniform initial concentrations $c_{O,i}$ and $c_{R,i}$, respectively, which are transported only by diffusion (with diffusion coefficient D) and react at the surface of the electrodes by exchanging n_e electrons.

$$O + n_e e^- \rightleftharpoons R \tag{1}$$

For the sake of simplicity, reversible electrode reactions are assumed, and therefore, the Nernst equation is valid even when the current flows through the electrodes [7].

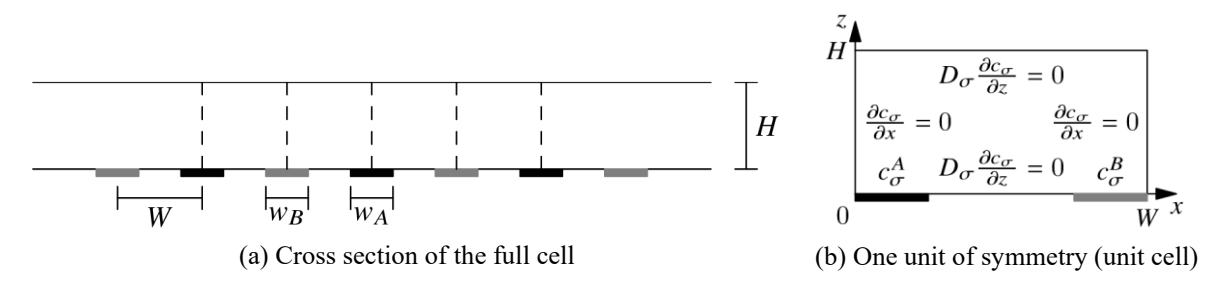


Figure 1. Shallow electrochemical cell with an IDAE. This cell can be regarded as an assembly of several unit cells. Here c_{σ} is the concentration of species σ (either O or R), and c_{σ}^{A} and c_{σ}^{B} are the concentrations applied at bands A and B, respectively

If the length L is sufficiently large, the fringing effects at the ends of each band can be neglected, and the electrochemical cell reduced to two dimensions. Moreover, if the number of bands is large enough, the fringing effects at both ends of the IDAE can also be neglected, allowing the IDAE to be represented as an assembly of two-dimensional $unit\ cells$ (Figure 1b) due to its periodic arrangement [4, 8]. In the event of a counter electrode external to the IDAE, this is assumed to be located far away, such that the fringing effects at both ends of the IDAE are further avoided.

Under these conditions, the concentration profile inside a single unit cell is given by the diffusion equation

$$\frac{1}{D}\frac{\partial c_{\sigma}}{\partial t} = \frac{\partial^{2} c_{\sigma}}{\partial x^{2}} + \frac{\partial^{2} c_{\sigma}}{\partial z^{2}}$$
 (2)

where $c_{\sigma}(x, z, t)$ is the concentration of species σ (either O or R), which is subject to the initial concentrations present in the electrochemical cell

$$c_{\sigma}(x,z,0^{-}) = c_{\sigma,i} \tag{3}$$

as well as boundary conditions for insulation (top and bottom), symmetry (left and right), and applied concentrations c_{σ}^{A} and c_{σ}^{B} at the bands, as indicated in Figure 1b.

It should be noted that the concentrations applied at the surface of the bands E (which can be either A or B) are uniform. This is possible due to the validity of the Nernst equation

$$ln\left(\frac{c_E^O}{c_E^B}\right) = \frac{Fn_e}{RT}(V_E - V^{o'}) \tag{4}$$

where F is Faraday's constant, R is the universal gas constant, T is the temperature of the system, V_E is the potential applied at bands E, and V° ' is the formal potential of the redox couple. Furthermore, the sum of concentrations at any point in the unit cell is constant and uniform [4, 8]

$$c_{O}(x,z,t) + c_{R}(x,z,t) = c_{O,i} + c_{R,i}$$

Both facts make the concentrations of species O and R at each band E (either A or B) uniform and dependent only on the potential applied at that same band

$$c_O^E = \frac{c_{O,i} + c_{R,i}}{\frac{-Fn_E}{RT}(V_E - V^{O_f})}$$
 (5)

$$c_R^E = \frac{\frac{c_{R,i} + c_{O,i}}{1 + e^{-RT}(V_E - V^{O_f})} \tag{6}$$

Once the concentration profile is known, the current at an individual band E (either A or B) can be obtained by integrating the current density on that band

$$i_E = \int_E \mp F \, n_e D \, \frac{\partial c_\sigma}{\partial z}(x, 0, t) L dx \tag{7}$$

where minus or plus signs should be used when the species σ corresponds to O or R, respectively.

Implementation of the simulations

All equations were normalized using the relations $\gamma_{\sigma} = [c_{\sigma} - c_{\sigma}{}^{A}]/[c_{\sigma}{}^{B} - c_{\sigma}{}^{A}], \ \xi = x/W, \ \zeta = z/W \ \text{and} \ \tau = \pi^{2}Dt/W^{2},$ to make the results available for devices fabricated at different scales. In particular, the diffusion equation, its initial concentration, and the concentrations at the bands were transformed to

$$\pi^2 \frac{\partial \gamma_\sigma}{\partial \tau} = \frac{\partial^2 \gamma_\sigma}{\partial \xi^2} + \frac{\partial^2 \gamma_\sigma}{\partial \xi^2} \tag{8}$$

$$\gamma_{\sigma}(\xi, \zeta, 0^{-}) = \gamma_{\sigma, i} = \frac{c_{\sigma, i} - c_{\sigma}^{A}}{c_{\sigma}^{B} - c_{\sigma}^{A}}$$

$$\tag{9}$$

$$\gamma_{\sigma}(\xi, 0, \tau) = 0 \text{ for } \xi \in A \tag{10}$$

$$\gamma_{\sigma}(\xi, 0, \tau) = 1 \text{ for } \xi \in B \tag{11}$$

while the boundary conditions for insulation and symmetry remained equal to zero, and the normalized current at a single band resulted in

$$\frac{i_E/L}{\pi^2 F n_e D \left[c_B^B - c_A^A \right]} = \int_E \frac{\mp 1}{\pi^2} \frac{\partial \gamma_\sigma}{\partial \zeta} (\xi, 0, \tau) d\xi \tag{12}$$

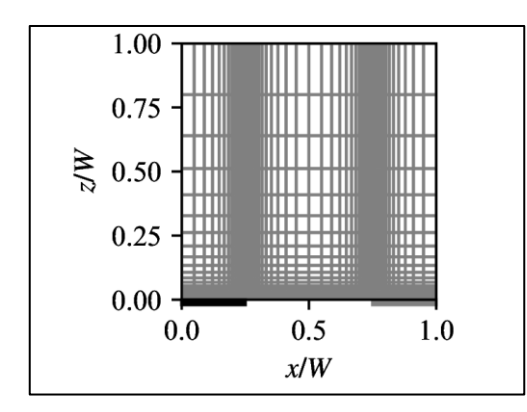
where minus or plus signs should be used when the species σ corresponds to O or R, respectively.

Two cases were considered for initial concentrations: (i) The case $\gamma_{\sigma,i} = 0$, where the initial concentration of one species equals the concentration applied at one of the arrays $c_{\sigma,i} = c_{\sigma}^A$. This is a common setup for IDAEs, especially when $c_{\sigma,i} = 0$ and the concentration c_{σ}^A is forced to zero by potentiostating at a fixed extreme potential [4], while the concentration at the other array c_{σ}^B is potentiostated at will. This configuration requires

a bipotentiostat with a counter electrode external to the IDAE.

(ii) The case $\gamma_{\sigma,i} = 0.5$, where the average concentration applied to the arrays is equal to the initial concentration $(c_{\sigma}^{A} + c_{\sigma}^{B})/2 = c_{\sigma,i}$. This condition, together with bands of equal width $(w_{A} = w_{B})$, produces symmetrical concentration profiles, leading to equal currents at the arrays [8, 9]. This last situation corresponds to the case where a conventional potentiostat drives one of the arrays while the other array performs as a counter electrode, thus sparing the need for an external counter electrode.

In particular, IDAEs with bands and gaps of equal width $(w_A = w_B = W/2)$ were considered for all simulations, since this is a common design choice, and also because it facilitates the display of results. This choice also simplifies the implementation of the meshes, chosen in this study to be of an exponential kind as shown in Figure 2. Each mesh used in the simulations consists of $n_x \times n_z$ elements, where the size of the smallest element is $\delta_x = \delta_z = \delta_0$, and the remaining elements increase in size according to the growth factor (stretching parameter) $r_x = r_z = r$ [10]. The resolution of the meshes was tested for diffusion in steady state with a unit cell with an aspect ratio H/W = 1 (Figure 2) and successively refined until the absolute error of the normalized current between two consecutive iterations was less than 0.0005, corresponding approximately to three decimal places of accuracy. The values obtained for the smallest element and the growth factor were $\delta_0 = 0.00025$ and r \approx 1.2496, respectively, and used for all simulations in this study.



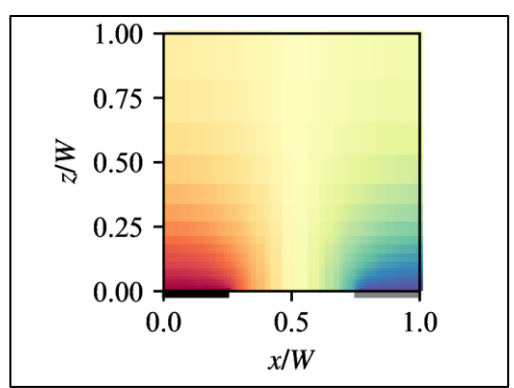


Figure 2. Exponential mesh (left) and normalized concentration in steady state (right) for the case H/W = 1. Number of elements is $n_x \times n_z = 100 \times 31$, and size of the smallest element $\delta_x = \delta_z = \delta_0 = 0.00025$ with a growth factor of $r_x = r_z = r \approx 1.2496$.

The simulations considered different aspect ratios $H/W = \{1, 1/2, 1/3, ..., 1/10\}$, and were solved numerically by writing the normalized diffusion equation, its boundary conditions, and the corresponding meshes in Python with the aid of the FiPy package [11]. These simulations can be downloaded from [12].

Exponential fits for the current response

The concentration profile in a shallow cell containing an IDAE evolves over time in a complex manner, with the addition of several Fourier harmonics to produce the right result. Each of these harmonics contains an exponential factor

$$exp\left(-\left[n^2+k^2\frac{W^2}{H^2}\right]\frac{\pi^2}{W^2}Dt\right) \text{ for } n=1,2,... \\ k=0,1,...$$
 (13)

which dampens the influence of the harmonic over time. Some of these harmonics will decay faster than others. In particular, the harmonic (n, k) = (1, 0) is the slowest to decay and the only one remaining and contributing to the concentration for times $\pi^2 Dt/W^2 > 1$ and aspect ratios H/W < 1/2. The exponential factors of all other harmonics $(n \ge 1$ and $k \ge 1)$ are less than $\exp(-[1^2 + 1^2 \times 2^2]) = \exp(-5) \approx 0.0067 = 0.67\%$ and therefore disappear quickly. This leads the concentration profile to behave like an exponential under the conditions stated previously [8].

The previous argument also suggests that the current may behave like an exponential after a certain time T

$$i_E = i_f + K \exp(-t/\tau_i) \quad \text{for } t \gtrsim T$$
 (14)

where i_f is the current of a single band in steady state, K is a real number, and τ_i is the *time constant* of the current response. However, this time T may not be equal to its counterpart obtained for the concentration.

After obtaining the time response of the current by numerically solving the diffusion equation, we searched for the time T and the parameters i_f , K and τ_i of the exponential curve. This was done in four steps (see Figure 3): (i) Search for the time t_{ss} where the current i_E and its steady state i_f differ by 0.67%. This gives a rough approximation of the time when an exponential decays to 0.67% (which corresponds to $5\tau_i$). (ii) Find the time $t_{ss}/5$. This gives a rough approximation of the time constant of the current τ_i . However, this time may be too soon for the current to behave exponentially. (iii) Find the time $T = 2t_{ss}/5$. This time gives a rough approximation of $2\tau_i$, where it is more likely for the current to start behaving exponentially. We could have also chosen $3t_{ss}/5$; however, $2t_{ss}/5$ gave good results for exponential fit. Times near $4t_{ss}/5$ or beyond are not advisable, since they would be too close to the time where the current reaches steady state, and thus the current would no longer be exponential but nearly constant. (iv) Once $T = 2t_{ss}/5$ is known, fit an exponential curve to the simulation data of the current between times T and t_{ss} to obtain the fitting parameters i_f , K, and τ_i . Since the model for the current is not linear

in its parameters, a non-linear fit needs to be performed. This procedure was also implemented in Python, whose script can be downloaded from [12].

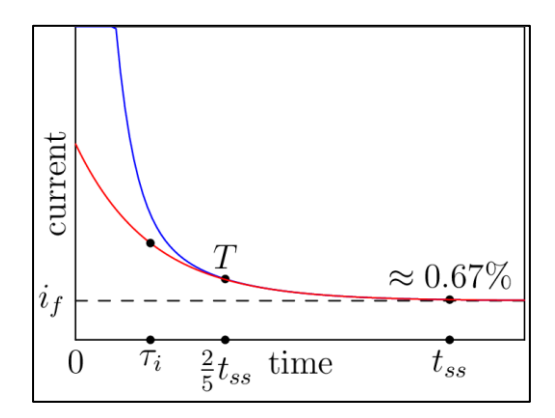


Figure 3. Process to obtain the exponential fit (red) for the time response of the current (blue). (i) Find t_{ss} , which corresponds to the time where the current i_E and i_f differ by 0.67%. (ii) Find t_{ss} /5, which gives a rough approximation of τ_i . (iii) Find $T = 2t_{ss}$ /5, which gives a rough approximation of the time $2\tau_i$. (iv) Fit an exponential curve to the time response of the current i_E , by taking the simulation data between $T = 2t_{ss}$ /5 and t_{ss}

Results and Discussion

The simulations of the currents and their respective exponential fits were performed for the cases involving external and internal counter electrodes, using a bipotentiostat and conventional potentiostat, respectively; the most common configurations to drive an IDAE. For both cases, electrochemical cells of different heights were used while fixing the width of the unit cell. The results are discussed below.

Case of external counter electrode ($c_{\sigma,i} = c_{\sigma}^A$)

For this case, we considered that the initial concentration of one species equals its concentration applied at one array $c_{\sigma,i} = c_{\sigma}^{A}$, achieved by potentiostating array A and forcing c_{σ}^{A} to be equal to $c_{\sigma,i}$, while array B is potentiostated at will. In practice, this requires the use of a bipotentiostat with a counter electrode external to the IDAE.

Under these conditions, several simulations were performed using different values of W/H. The simulations produced currents of different magnitude at bands A and B, as shown in Figure 4. This provides clear evidence of the need for a counter electrode, external to the IDAE, to be responsible for collecting the net current

 $i_{\text{net}} = i_A + i_B \neq 0$ produced in every unit cell, as indicated in Figure 5. However, as the simulations reach steady state, the net current tends to zero, meaning that the currents at both bands must be balanced in steady state $i_A = -i_B$. This is only possible under the assumption of a large number of bands and an external counter electrode far away from the IDAE.

As expected, all currents obtained by simulation (circles) can be approximated by exponentials (lines), as presented in Figures 4 and 5. In fact, in the case of currents at B in Figure 4, the exponential approximations show some deviation from their simulated counterparts for $t > \tau_i$, while improving considerably for t > T (where T is roughly $2\tau_i$), and clearly showing a steady-state response for $t > 5\tau_i$. The parameters i_f , K, and τ_i obtained from all exponential fits are given in Table 1, such that the exponential approximations can be easily reconstructed as required.

In Figure 6, the magnitudes of currents at A and B are equal in steady state and decrease as the cell becomes shallower. This is because there are two main gradients

of concentration when the electrochemical cell is tall: (i) between the IDAE and the bulk concentration near the roof of the cell; and (ii) in between consecutive bands (Figure 2). However, when the cell becomes shallower, the gradient between the IDAE and the roof of the cell tends to disappear, leaving only the gradient of concentration between consecutive bands. The time constants of currents at *A* and *B*, as well as the net current, are all equal, decreasing as the cell becomes shallower. This is because the electrochemical species can escape to the region of bulk concentration near the roof of the cell when the cell is tall (Figure 2) and later diffuse to the external counter electrode. However, when

the cell becomes shallower, the electrochemical species are forced to diffuse only between consecutive bands due to the low roof of the cell. Therefore, in the case of a shallow cell, the species diffuse through a shorter distance compared to the case of a taller cell.

The previous results show that there is a compromise between sensitivity (current) and response time (time constant) of the sensor. The taller the electrochemical cell, the more sensitive it becomes, but the longer the response time. Conversely, the shallower the electrochemical cell, the less sensitive it becomes, but the shorter the response time.

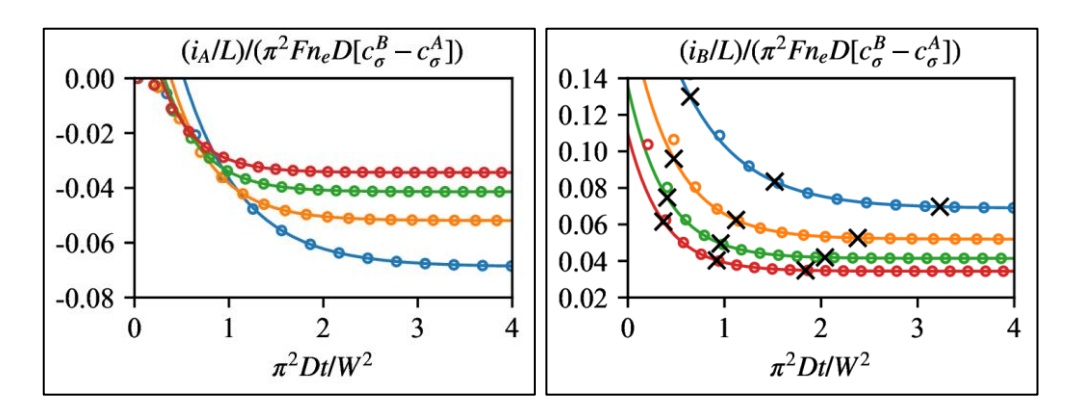


Figure 4. Normalized versions of the current through single bands i_A (left) and i_B (right) for selected aspect ratios W/H = {4, 6, 8, 10} (lines in order from blue to red) and initial concentration $c_{\sigma,i} = c_{\sigma}^A$. Circles correspond to the simulation points, while solid lines correspond to the exponential fit. Crosses on a line correspond to the times τ_i , T and $5\tau_i$ (in order from left to right)

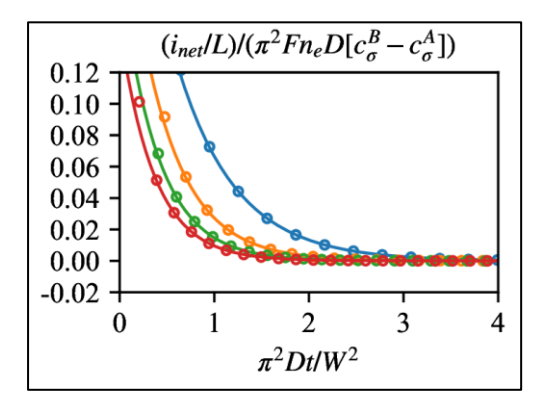


Figure 5. Normalized version of the net current $i_{net} = i_A + i_B$ for selected aspect ratios $W/H = \{4, 6, 8, 10\}$ (lines in order from blue to red) and initial concentration $c_{\sigma,i} = c_{\sigma}^A$. Circles correspond to the simulation points, while solid lines correspond to the exponential fit

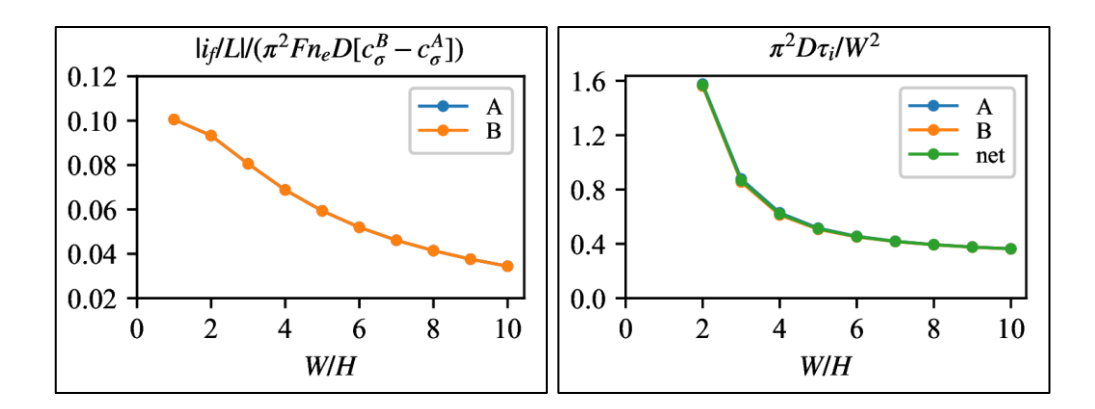


Figure 6. Normalized versions of the absolute value of the steady-state current $|i_f|$ (left) and the time constant of the current τ_i (right) for different aspect ratios W/H and initial concentration $c_{\sigma,i} = c_{\sigma}^A$. The case W/H = 1 has been omitted from the normalized time constant plot to maintain good visualization of the lower values

Table 1. Parameters resulting from the exponential fit of normalized currents for different aspect ratios W/H and initial concentration $c_{\sigma,i} = c_{\sigma}^{A} = 0$. The parameters p_0 , p_1 , and p_2 correspond to the normalized versions of i_f , K and τ_i , that is, $(i_f/L)/(\pi^2 F n_e D[c_{\sigma}^{A} - c_{\sigma}^{B}])$, $(K/L)/(\pi^2 F n_e D[c_{\sigma}^{A} - c_{\sigma}^{B}])$, and $\pi^2 D \tau_i / W^2$. The coefficient of determination was $R^2 > 0.9999$ for all cases

		\boldsymbol{A}			В			net	
W/H	<i>p</i> ₀	p 1	p ₂	p ₀	p 1	p ₂	p_0	p 1	p ₂
1	-0.1005	0.0878	5.1005	0.1005	0.0878	5.1002	0	0.1757	5.1003
2	-0.0933	0.1447	1.5761	0.0933	0.1446	1.5611	0	0.2943	1.5685
3	-0.0806	0.1643	0.8779	0.0806	0.1820	0.8549	0	0.3459	0.8662
4	-0.0688	0.1581	0.6287	0.0688	0.1759	0.6118	0	0.3336	0.6201
5	-0.0593	0.1406	0.5156	0.0593	0.1506	0.5065	0	0.2910	0.5110
6	-0.0519	0.1215	0.4554	0.0519	0.1266	0.4505	0	0.2480	0.4529
7	-0.0461	0.1054	0.4191	0.0461	0.1079	0.4165	0	0.2133	0.4178
8	-0.0414	0.0925	0.3945	0.0414	0.0941	0.3927	0	0.1865	0.3936
9	-0.0376	0.0823	0.3769	0.0376	0.0834	0.3756	0	0.1657	0.3763
10	-0.0344	0.0742	0.3638	0.0344	0.0749	0.3630	0	0.1491	0.3634

Case of internal counter electrode $(c_{\sigma,i} = [c_{\sigma}^A + c_{\sigma}^B]/2)$ In this case, the average concentration applied at the bands equals the initial concentration $(c_{\sigma}^A + c_{\sigma}^B)/2 = c_{\sigma,i}$, corresponding to the case where a conventional potentiostat drives one of the arrays while the other array performs as a counter electrode. Here, the potential (and therefore the concentration) of the counter electrode is

regulated automatically by the potentiostat following the previous average condition, which can be rewritten as $[c_{\sigma}^{A} - c_{\sigma,i}] = -[c_{\sigma}^{A} - c_{\sigma,i}].$

Under these conditions, several simulations were performed using different values of W/H. Unlike the case of the external counter electrode, these simulations

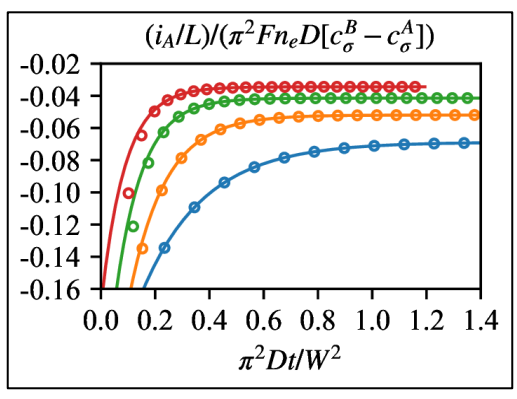
produced currents of the same magnitude at bands A and B, but with the opposite sign $i_A = -i_B$, and not only during steady state but for all simulation times (Figure 7). This means that all current generated by bands B is always collected by bands A, thus confirming the use of an internal counter electrode.

As before, all currents obtained by simulation (circles) can be approximated by exponentials (lines), as presented in Figure 7. For example, in the case of currents at bands B, the exponential approximations show some deviation for times $t > \tau_i$, but a considerable improvement for t > T (roughly $2\tau_i$). All current responses reach steady state at times $t > 5\tau_i$. The parameters i_f , K, and τ_i obtained from all exponential fits are given in Table 2, such that the exponential approximations can be easily reconstructed as required.

In Figure 8, the magnitudes of the currents at bands A and B decrease as the cell becomes shallower, in the same way as in the case of the external counter electrode

(at least for their normalized versions). In similarity to the case of the external counter electrode, this is due to the vertical gradient of concentration between the IDAE and the roof of the cell (Figure 2), which disappears as the cell becomes shallower. The time constants of the currents at bands A and B are equal, decreasing as the cell becomes shallower. However, the values obtained here are much shorter than those obtained for the external counter electrode (compared with Figure 6). This can be explained by the absence of an external counter electrode, and therefore, the species cannot escape far from the IDAE but diffuse only between consecutive bands, even in the case of a tall electrochemical cell.

Finally, as in the case of the external counter electrode, a compromise exists between the sensitivity (current) and response time (time constant) of the electrochemical sensor. The shallower the electrochemical cell, the less sensitive it becomes, but the shorter the response time. And vice versa in the case of tall cells.



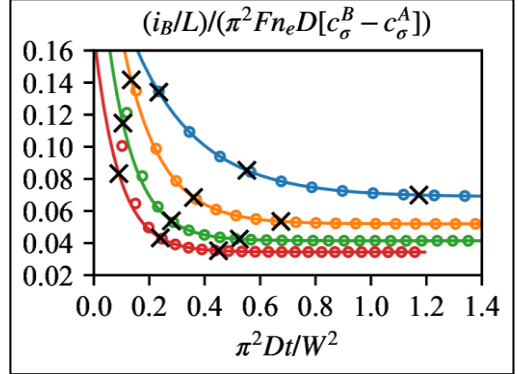
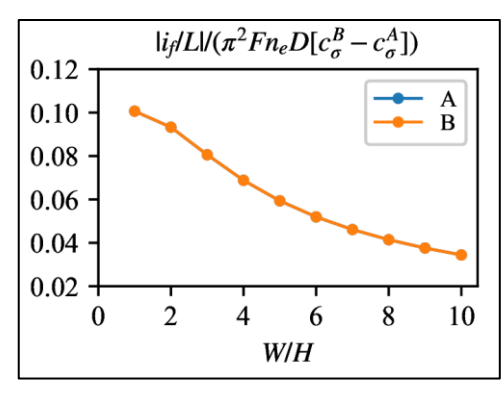


Figure 7. Normalized versions of the current through single bands i_A (left) and i_B (right) for selected aspect ratios W/H = {4, 6, 8, 10} (lines in order from blue to red) and initial concentration $c_{\sigma,i} = (c_{\sigma}^A + c_{\sigma}^B)/2$. Circles correspond to the simulation points, while solid lines correspond to the exponential fit. Crosses on a line correspond to the times τ_i , T, and $5\tau_i$ (in order from left to right)



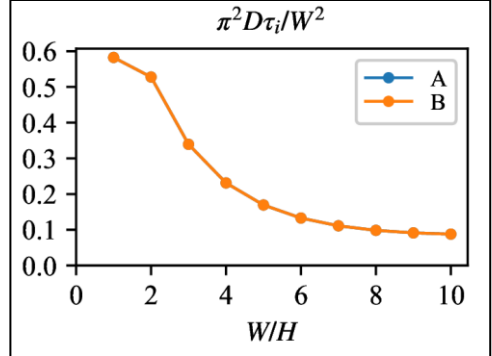


Figure 8. Normalized versions of the absolute value of the steady-state current $|i_f|$ (left) and the time constant of the current τ_i (right) for different aspect ratios W/H and initial concentration $c_{\sigma,i} = (c_{\sigma}^A + c_{\sigma}^B)/2$

Table 2. Parameters resulting from the exponential fit of normalized currents for different aspect ratios W/H and initial concentration $c_{\sigma,i} = (c_{\sigma}^A + c_{\sigma}^B)/2$. The parameters p_0 , p_1 , and p_2 correspond to the normalized versions of i_f , K, and τ_i , that is, $(i_f/L)/(\pi^2 F n_e D[c_{\sigma}^A - c_{\sigma}^B])$, $(K/L)/(\pi^2 F n_e D[c_{\sigma}^A - c_{\sigma}^B])$, and $\pi^2 D \tau_i/W^2$. The coefficient of determination was $R^2 > 0.9985$ for all cases

		\boldsymbol{A}		В			
W/H	p 0	p 1	p 2	p 0	p 1	p ₂	
1	-0.1006	-0.0310	0.5825	0.1006	0.0310	0.5825	
2	-0.0933	-0.0601	0.5277	0.0933	0.0601	0.5277	
3	-0.0806	-0.1212	0.3392	0.0806	0.1212	0.3392	
4	-0.0688	-0.1800	0.2312	0.0688	0.1800	0.2312	
5	-0.0593	-0.2253	0.1694	0.0593	0.2253	0.1694	
6	-0.0519	-0.2479	0.1328	0.0519	0.2479	0.1328	
7	-0.0461	-0.2426	0.1111	0.0461	0.2426	0.1111	
8	-0.0414	-0.2132	0.0984	0.0414	0.2132	0.0984	
9	-0.0376	-0.1739	0.0913	0.0376	0.1739	0.0913	
10	-0.0344	-0.1363	0.0877	0.0344	0.1363	0.0877	

Conclusion

In this work, the main issue of whether the current response of an IDAE in a shallow electrochemical cell can be modeled by an exponential function has been addressed. The results show that a simple exponential function can approximate the time response of the current for elapsed times greater than approximately two-time constants, reaching steady state after approximately five-time constants. Normalized steady-

state currents and time constants were tabulated for different aspect ratios (separation between bands with respect to height of the cell), such that they can be used for cells of different scales or dimensions.

When driving the IDAE with a bipotentiostat (both arrays perform as working electrodes), the net current at the arrays is non-zero during the transient state (approaching zero in steady state) and must be collected

by an external counter electrode. On the other hand, when driving the IDAE with a conventional potentiostat (one array performs as a working electrode, while the other performs as an internal counter electrode), the currents at the arrays are always of equal magnitude and opposite signs (during the transient and steady states).

In the cases of external and internal counter electrodes, the steady-state magnitude and time constant of the current decrease as the electrochemical cell becomes shallower. This shows a trade-off or compromise between sensitivity (in terms of current magnitude) and response time (in terms of time constant) for IDAEs in shallow cells. Higher currents can be obtained at the expense of longer response times when the cell is tall (compared to the separation between consecutive bands of the IDAE) and shorter response times at the expense of lower currents when the cell is shallow.

Acknowledgment

The authors gratefully acknowledge *Petchra Pra Jom Klao Ph.D. Scholarship* (Grant No. 28/2558), *King Mongkut's University of Technology Thonburi*. The authors also acknowledge the financial support provided by *King Mongkut's University of Technology Thonburi* and the *Research Network NANOTEC* (RNN) program (Grant No. P1851883) of the *National Nanotechnology Center* (NANOTEC), NSTDA, Ministry of Science and Technology, Thailand.

References

- 1. Karimian, N. and Ugo, P. (2019). Recent advances in sensing and biosensing with arrays of nanoelectrodes. *Current Opinion in Electrochemistry*, 16: 106-116.
- Rackus, D. G., Shamsi, M. H. and Wheeler, A. R. (2015). Electrochemistry, biosensors and microfluidics: A convergence of fields. *Chemical Society Reviews*, 44: 5320-5340.
- Gencoglu, A. and Minerick, A. R. (2014). Electrochemical detection techniques in micro- and nanofluidic devices. *Microfluidics and*

- Nanofluidics, 17: 781-807.
- Aoki, K., Morita, M., Niwa, O. and Tabei, H. (1988). Quantitative analysis of reversible diffusion-controlled currents of redox soluble species at interdigitated array electrodes under steady-state conditions. *Journal of Electroanalytical Chemistry and Interfacial Electrochemistry*, 256, 269-282.
- Kanno, Y., Goto, T., Ino, K., Inoue, K. Y., Takahashi, Y., Shiku, H. and Matsue, T. (2014). SU-8-based flexible amperometric device with IDA electrodes to regenerate redox species in small spaces. *Analytical Sciences*, 30: 305-309.
- Heo, J.-I., Lim, Y. and Shin, H. (2013). The effect of channel height and electrode aspect ratio on redox cycling at carbon interdigitated array nanoelectrodes confined in a microchannel. *Analyst*, 138: 6404-6411.
- Oldham, K. and Myland, J. (1994). Fundamentals of electrochemical science. Academic Press, UK. §5:8.
- 8. Guajardo, C., Ngamchana, S. and Surareungchai, W. (2013). Mathematical modeling of interdigitated electrode arrays in finite electrochemical cells. *Journal of Electroanalytical Chemistry*, 705: 19-29.
- Morf, W. E., Koudelka-Hep, M., de Rooij, N. F. (2006). Theoretical treatment and computer simulation of microelectrode arrays. *Journal of Electroanalytical Chemistry*, 590: 47-56.
- 10. Britz, D. and Strutwolf, J. (2016). Digital simulation in electrochemistry. Springer International Publishing, Switzerland. §7.2.
- Guyer, J. E., Wheeler, D. and Warren, J. A. (2009).
 FiPy: Partial differential equations with Python.
 Computing in Science and Engineering, 11(3): 6-5.
- 12. Guajardo Y., Cristian F. and Surareungchai, W. (2021). Simulations for the current's time response of interdigitated arrays in shallow electrochemical cells using FiPy. https://doi.org/10.5281/zenodo.5633322 [software].